AO13: Estimating the height of volcanic clouds using geostationary satellite and wind data

Author: Joseph Powell

Supervisors: Dr I. Taylor and Professor R. Grainger

Abstract

The height of a volcanic cloud is a key parameter that can be used to predict the evolution of the cloud, and its climatic impact. Two methods for estimating the height of volcanic clouds are tested. In both methods, the speed and direction of motion of volcanic clouds are calculated using images from the Spinning Enhanced Visible Infra-Red Imager (SEVIRI) and compared to the European Centre for Medium-Range Weather Forecasts' (ECMWF) reanalyses of the horizontal wind speed components with altitude at the volcano location. An intersection method and goodness method are used to estimate the cloud-top height of volcanic clouds produced by eruptions from Mt Etna on 28/02/2021 and 07/03/21.

Both methods are found to provide good height estimates that agree with local volcanism reports in the second hour following initial ash detection. However, both methods produce either inaccurate or very uncertain height estimates in the first 30-45 minutes post ash detection. The goodness method, which produces a colour map demonstrating the likelihood that a height is that of the volcanic cloud, is found to have fewer limitations and be the more informative method.

1 Introduction

1.1 Background

Volcanic emissions have significant near-term impacts on aviation, respiratory health, and water pollution, and therefore pose a considerable health and economic threat. For example, the 2010 Eyjafjallajökull eruption was estimated to have caused a net loss of US$ 2.2 billion to the aviation industry alone [1]. Furthermore, the sudden eruptions of Chaitén, Chile in May 2008, which produced plumes reaching up to 30 km altitudes [2], represented a dangerous increase in fine ash and aerosol amounts for distances as large as 100 km away from the volcano, for up to a month [3]. These cases indicate the need for a fast method for volcanic emission detection, and subsequent monitoring, to mitigate any physical and financial damage.

Additionally, fine ash and aerosols produced by volcanic eruptions can induce tropospheric cooling effects, whose impact is determined by factors such as the injection height, particle size distribution, and total mass injected. In particular, stratospheric ash has been found to persist on the scale of months to a year, unlike tropospheric ash injections [4]. This could lead to greater cooling for longer periods. Hence, understanding the height distribution of a volcanic cloud post-eruption is crucial to enable accurate modeling of volcanic perturbations on climate change from the current global warming trend.

1.2 Remote Sensing and Motivation

Satellite remote sensing has become an increasingly more reliable data source for volcanic plume detection and the study of plume-to-cloud evolution with time, particularly compared to ground-based detection methods. Not only are ground-based observations laborious, time-intensive, and potentially dangerous to gather, but satellite imagery can capture the entire geographical scale of the evolution (over hours or days) of the cloud. This simplifies the comparison of ash profiles between images taken at regular time intervals by the instrument.

In this project, the volcanic cloud is tracked by following the ash produced in the eruption because these particles are produced in significant quantities and ash is easily characterised using SEVIRI's spectral channels. Additionally, previous work by Taylor et al. [5] has demonstrated the potential for using ash images and wind profiles to estimate the height of volcanic clouds. Taylor et al. used the Advanced Baseline Imager (ABI) to test whether

the cloud was more likely to be in the troposphere or stratosphere by comparing local wind profiles to the ash data from true/false colour images taken at 1-10 minute intervals.

This project builds on the work by Taylor et al. by testing two methods, based on the fundamental concept of comparing wind profiles with the ash motion, for more precise volcanic cloud height estimation on two eruptions of Etna in 2021. The Etna case eruptions are selected for ease of access to the local wind profiles via the ECMWF, the simplicity of the characteristics of the eruptive events relative to the April 2021 eruption of La Soufrière [5], and the desire to showcase the potential of the height estimation method in wind-driven regimes, while transparently communicating its limitations. These eruptions are dated 28/02/21 and 07/03/21, while an eruption dated 10/03/21 is used to convey one of the pitfalls of the current ash detection method in appendix A.

A comparison of wind data against ash images taken by SEVIRI at fifteen minute intervals enables close testing of the plume response to the local wind profile and aims to increase the precision of the height estimation. In particular, the direction of ash motion and the ash speed will be compared to the local wind bearing and speed profiles in an attempt to obtain consistent height estimations across multiple variables. The use of geostationary satellite data also implies the potential for future application of this method for real-time plume evolution predictions.

2 Methods

2.1 Ash Observation with SEVIRI

Before any height estimation can be performed, images of the volcanic ash cloud must be obtained. The SEVIRI instrument is a radiometer that measures the top of atmosphere radiance from the atmosphere across 12 different spectral bands. This includes the narrow 10.8 μm infrared wavelength channel, which integrates the radiance in the 9.80 - 11.8 μm spectral interval [6]. Mt Etna (37.75° N, 14.99° E) is a good candidate for the application of this method using SEVIRI because it lies close to the centre of SEVIRI's observed area of -81 to 81° N and -79 to 79° E. In spite of this, spatial resolution at Etna is worse than its sub-satellite point resolution of 3 km x 3 km, and parallax at this latitude and longitude becomes a significant source of error in the difference between the ash cloud positions as the plume rises.

The 10.8 μm channel is chosen for volcanic cloud detection because the ash absorption feature has a characteristic 'V-shape' that extends through this channel, making SEVIRI a suitable instrument. Furthermore, the 9.80 - 11.8 μm spectral interval lies close to the 10-12 μm wavelength channel used by Prata [7] to characterise ash presence in an atmospheric column. The ash absorption feature partially sits in an atmospheric window, meaning that other clouds or dust can produce false ash detection.

2.2 Ash Detection

Atmospheric columns that contain ash are defined in the SEVIRI brightness temperature (BT) images by flagging pixels that have BTs below some predefined BT threshold, as demonstrated in figure 1. In this context, brightness temperature is simply the temperature of a blackbody that emits the same amount of radiation in the wavelength range of interest as has been measured by the instrument. Hence, pixels with lower BTs are likely to contain more ash because the ash will absorb radiation emitted from the Earth's surface in the 10.8 μm channel, lowering the amount of radiation reaching the detector.

This detection method limits its computational cost by defining narrower latitude and longitude scene ranges for the image analysis. These are 35 to 40° N, 13 to 18° E for the 28/02/21 eruption; and 36 to 40° N, 14 to 20° E for the 07/03/21 eruption. A BT threshold of T_{thresh} = 250 K is used for the 28/02/21 eruption and T_{thresh} = 230 K for the 07/03/21 eruption. These ranges and thresholds are chosen to avoid mistakenly flagging other particulates or cloud types as ash.

Ash clouds can often be detected using such low BT thresholds because of their high optical thickness; for the same reason, the presented method provides an estimate for the height of the top of the volcanic cloud specifically. The scenes in this study are only representative of scenes that contain limited non-volcanic cloud cover because this ash detection method cannot distinguish volcanic from non-volcanic clouds. See appendix A for evidence of this. As our analysis relies on the assumption that all flagged pixels contain ash, more thorough ash detection methods are recommended for future work. This limitation, along with others

associated with the methods presented, is listed in table 1. Other ash detection methods include the reverse absorption method [7], or the temperature gradient method [8].

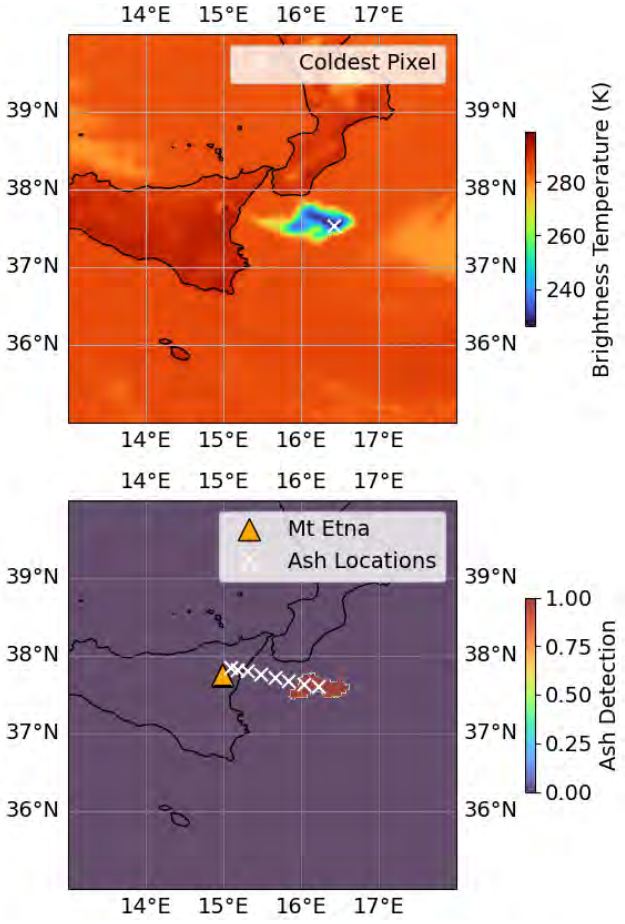

Figure 1: The loaded scene near Etna at 09:45 UTC on 28/02/21. Top: The BT image plotted from SEVIRI's dataset. Bottom: The image of pixels flagged for ash using T_{thresh} = 250 K.

2.3 Quantifying the Ash Motion

Equipped with images of flagged ash pixels at fifteen minute intervals, the direction and speed of the ash cloud can now be calculated. These are calculated by direct comparison of the ash locations in the two most recent images as the scene progresses in time. Firstly, average ash cloud locations, denoted in the bottom image of figure 1 by white crosses, are obtained for each image by averaging over the locations of the flagged pixels in each image. The angular direction of ash travel is defined as a forward bearing, which is a surface angle from the average ash location of image n to image n+1 taking north as 0°, taken at image n's ash location. This is an important distinction, as bearings do not remain constant as one travels in a straight line (that is, straight as perceived on the surface of Earth) across the surface of a spherical geometry. The ash locations in terms of latitudes ϕ_i and longitudes λ_i can be converted to a forward bearing β using equation (1), where $\Delta\lambda = \lambda_2 - \lambda_1$:

$$\beta = \arctan\left(\frac{\sin\Delta\lambda\cos\phi_2}{\cos\phi_1\sin\phi_2 - \sin\phi_1\cos\phi_1\cos\Delta\lambda}\right). \tag{1}$$

In order to calculate the shortest surface distance d between the two ash locations, the haversine equation (2) is used:

$$\begin{aligned} a &= \sin^2(\tfrac{\Delta\phi}{2}) + \cos\phi_1\cos\phi_2\sin^2(\tfrac{\Delta\lambda}{2}), \\ d &= 2R\arctan(\tfrac{\sqrt{a}}{\sqrt{1-a}}). \end{aligned} \tag{2}$$

Subsequently, the ash speed is calculated simply as $v = \frac{d}{t}$, assuming a constant ash speed v between images and a time interval t = 15 minutes. However, the Earth is an oblate spheroid, which means that the Earth radius R varies with latitude in the haversine formula where the haversine formula assumes a spherical geometry. The latitude-dependent Earth radius is calculated using equation (3), where R_e = 6378.137 x 10^3 m is the equatorial radius at sea level, R_p = 6356.752 x 10^3 m is the polar radius at sea level [9] and the latitude of the ash cloud is taken as that in the first image ϕ_1 on each time iteration, n:

$$R = \sqrt{\frac{(R_e^2\cos\phi_1)^2 + (R_p^2\sin\phi_1)^2}{(R_e\cos\phi_1)^2 + (R_p\sin\phi_1)^2}}. \tag{3}$$

Calculating the local Earth radius decreases the uncertainty introduced by assuming the Earth to be spherical. This can be further reduced by observing the cloud with finer time intervals. This reduces the difference in the Earth's radius $\Delta R = R_2 - R_1$ between each pair of sequential ash locations, assuming that there is latitudinal ash movement, and thus reduces the uncertainty in the ash forward bearing and speed. The scene used to observe the ash clouds from Etna until late-time dispersal has a latitudinal range of ~5°, resulting in an approximate 0.03% uncertainty contribution to the ash bearing and speed.

2.4 Wind and Temperature Profiles

The ECMWF Reanalysis v5 (ERA5) provides hourly estimates of meteorological variable profiles, such as temperature and horizontal wind

speed component profiles, with global coverage [10]. The ERA5 obtains its estimates by combining records of Earth observations with short-range forecasts based on the state of the Earth according to the reanalysis from the hour prior. Currently, ERA5 publishes its reanalysis results with a 5 day lag behind real-time. This means that, while near real-time volcanic height estimation using this data is not currently possible, this paper demonstrates the potential application of such an analysis. The ERA5 profiles have been temporally interpolated to match the 15 minute intervals of the data taken by SEVIRI because ERA5 only has hourly temporal resolution.

Once these profiles have also been spatially interpolated to the location of Etna, they can be plotted to demonstrate the expected ash motion at each height, assuming that the ash is in thermal equilibrium with its surroundings and the ash is strongly coupled to the local wind. Examples of wind and temperature profiles can be found in figures 2 and 3 respectively. The maximum height of the profile data considered for height estimation is limited to 20 km above the surface radius estimated by the model at that latitude to reflect the infeasibility of the cloud reaching heights above this. See the ERA5 documentation [11] for more details.

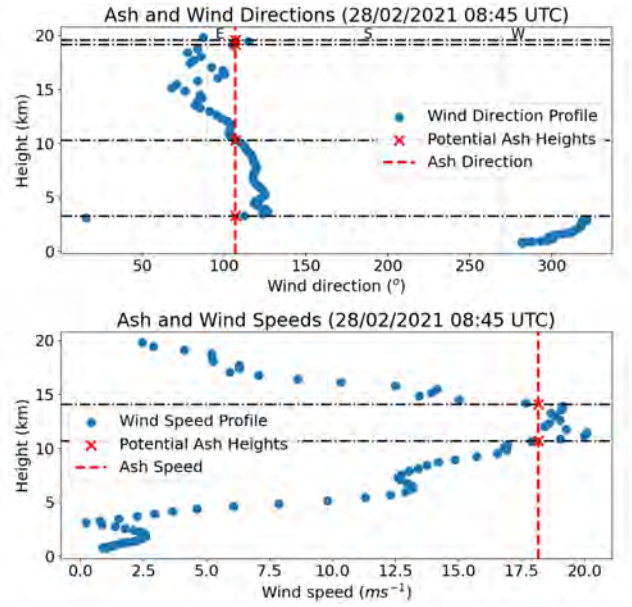

Figure 2: The ash direction of travel and speed plotted over the wind profiles from ERA5, interpolated in time and location to Etna at 08:45 UTC on 28/02/21. Intersections between these data are shown as red crosses, and constitute height estimates for this method. Top: Wind forward bearing profile plotted with ash direction to find height estimations based on wind direction. Bottom: Wind speed profile plotted with ash speed to find height estimations based on wind speed.

2.5 The Intersection Method

Two methods for obtaining estimates of the volcanic cloud height were explored. The first finds intersections between the ash speed / direction of travel, and the ERA5 wind profiles, taking these intersections to be candidate ash height estimates at a given time. Henceforth, this method shall be referred to as the intersection method. The method can be seen in practice in figure 2, where the black horizontal lines show the heights at which the blue wind profile intersects the red ash parameter. However, figure 2 also conveys that for wind profiles that vary little with height, this can produce a broad range of candidate height estimates, many of which are not sensible.

The most suitable intersection height for the timestep is picked by comparing these intersection heights with a single height produced by the brightness temperature (BT) method. The BT method is the most suitable comparative method because the height estimates can be generated using the same data sources and workflow for a more direct comparison. Furthermore, the BT method is commonly used to retrieve volcanic cloud heights [5][12] and, for the temperature profiles at the time and dates of interest, it often produces one sub-tropopause height estimate per timestep. However, often multiple solutions are produced because the Earth's temperature profile is non-monotonic and variable. Consequently, the BT method is subject to similar limitations, summarised by Taylor et al. [5], to the intersection method. Although the BT method relies on the assumption that the volcanic cloud is in thermal equilibrium with the ambient air at that height, which causes inaccuracies in estimates early after ash settles at the level of neutral buoyancy (LNB), a comparison is still useful to narrow the pool of realistic height estimates.

The BT method height estimates are found by comparing the BT of the coldest BT pixel in each scene to the temporally interpolated ERA5 temperature profile located at Etna. The height at which the coldest pixel temperature intersects the temperature profile, as shown in figure 3, is used to pick out the single closest height per timestep from the wind direction and wind speed analy-

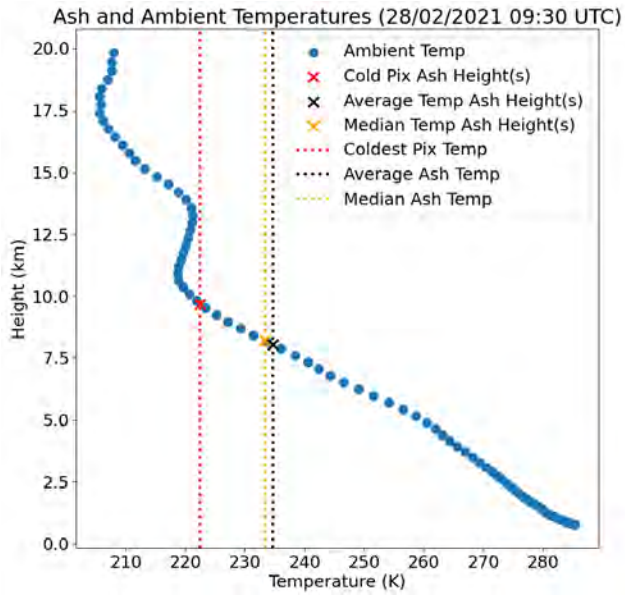

Figure 3: The coldest, average and median temperature of flagged pixels plotted over the ERA5 temperature profile at Etna interpolated in time to 9:30 UTC on 28/02/21. Crosses indicate the intersections between the temperature profile and each of the listed temperatures, constituting height estimates using the BT method. Pixels were flagged under the BT threshold $T_{thresh} = 250$ K.

ses. These selected heights are plotted alongside the coldest pixel heights as a time series in figure 5 for both case eruptions. It should be expected that more accurate height estimations would be obtained following the initial eruptive period, once the cloud height is roughly constant at the LNB but before the ash cloud begins to disperse under different wind profile regimes.

2.5.1 Uncertainties

The uncertainties in the heights are calculated differently for the two height estimation methods. In the intersection method the root mean square (rms) uncertainty in the selected height estimates for a particular parameter, either ash BT, speed, or direction, across all timesteps is used. That is, selected height estimates across all timesteps are plugged into equation (4) to produce the rms uncertainty, δh, for all height estimates produced by the comparison for that particular ash cloud parameter:

$$\delta h = \sqrt{\frac{\sum_{t=1}^{N}(h_t - \bar{h})^2}{N}}. \tag{4}$$

The N represents the number of timesteps of the ash cloud in the analysis, h_t is the height estimate produced by a particular ash cloud parameter comparison that lies closest to the coldest pixel height at timestep t, and $\bar{h}$ represents the mean of the selected heights across all timesteps produced by a particular parameter comparison.

2.6 The Goodness Method

The second method for estimating volcanic cloud heights involves defining a goodness parameter that determines how well a particular data point in the ERA5 wind profile matches the ash direction or speed from the BT scene. Henceforth, this method is referred to as the goodness method. The goodness, G, of a data point is defined in equation (5), where W is an array containing the speed or direction values of the wind profile at each recorded height, S is the ash speed or direction calculated from the BT image for that timestep, and δW and δS are the uncertainties associated with each of these values, respectively:

$$G = \frac{(W - S)^2}{(\delta W)^2 + (\delta S)^2}. \tag{5}$$

The uncertainties δW and δS are discussed further in section 2.6.1. The goodness treatment above is akin to a least squares treatment of the wind profile to the ash parameter. That is, lower goodness values at a particular height indicate that it is a good candidate for the ash height, and these lower goodness values occur at heights where the wind profile is closer to intersecting the ash speed or direction. Therefore, a height estimate is always produced, where the intersection method may not have produced a candidate, as in figure 4.

The goodness method gives the user a qualitative sense of the uncertainty in any height estimates, and by extension the suitability of the method for finding the volcanic cloud height, by outputting the goodness of data points across the full height range of interest. For example, the wind speed profile in figure 4 shows that a high goodness would be produced at heights below 10 km because it lies far from the ash speed value, as indicated by the orange arrow. However, similar goodness values in the 10-17 km altitude range would be produced, with the smallest of those being at the heights indicated by the black arrows. In this case, the user knows that the height they derive from these results will have a large uncertainty range spanning roughly 7 km.

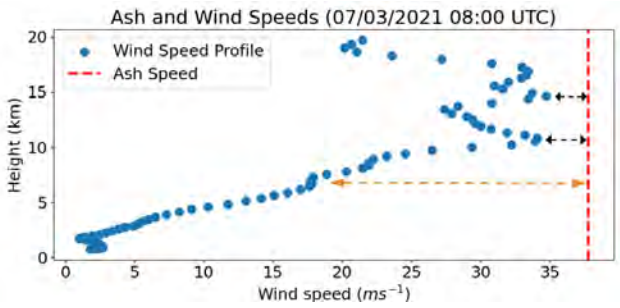

Figure 4: The ash speed plotted over the wind profile from ERA5, spatially interpolated to Etna at 08:00 UTC on 07/03/21. Arrows indicate the size of (W - S) used to calculate G_{spd} at different heights.

The total goodness value, G_{tot}, for a particular height is found by combining the goodness value from the wind-to-ash speed comparison, G_{spd}, with the goodness value from the wind-to-ash direction comparison, G_{dir}, in quadrature:

$$G_{tot} = \sqrt{G_{spd}^2 + G_{dir}^2}. \tag{6}$$

Using equation (6) ensures that any height estimates produced are well-informed by the data, while highly weighting agreement between the different parameters for height estimation in the resultant height estimate. The total goodness values for each height data point in the ERA5 wind profiles per timestep are presented as a logarithmically scaled colour map, as seen in figure 6. This scaling most effectively highlights the low goodness regions, and plotting as a colour map allows the user to easily interpret the qualitative changes to the ash height with time.

2.6.1 Uncertainties

In the goodness method, uncertainties in the ERA5 wind profiles, δW, and the ash cloud parameters, δS, directly influence the heights deemed most likely to be the ash cloud height through equation (5). δW is calculated as the rms uncertainty of each data point in the wind profile across all timesteps for a particular height. The δS for ash direction is obtained by considering the uncertainty in the pixel positions of the BT image and the uncertainty introduced by assuming that the Earth is spherical in the haversine formula (2). The uncertainty associated with the pixel positions in the BT image is taken as half of the sub-satellite surface pixel resolution, that is 1.5 km in the northward and eastward directions. Therefore, δS for the ash direction and speed will inevitably be an underestimated uncertainty because Etna lies at a latitude of 37.75° N, where the shallower angle to the satellite results in a larger pixel resolution.

The pixel size and Earth radius uncertainties, the latter being taken as R_e - $R_p \approx 21$ km, are propagated through the haversine equation (2) and forward bearing equation (1) as demonstrated in appendix B. This produces the uncertainty in the forward bearing, $\delta\beta$, which is equivalent to δS for the ash direction goodness, G_{dir}.

The percentage uncertainty associated with the pixel size (∼7.5%) is much larger than the percentage uncertainty associated with the Earth's radius (∼0.3%). Hence, δS for the ash speed is found by scaling the pixel-size uncertainty according to $v = \frac{d}{t}$, neglecting the uncertainty associated with the Earth's radius. The δS for the ash speed is then used to calculate G_{spd} according to equation (5). The subsequent colour map of G_{tot} is directly informed by the uncertainties associated with the ash and wind parameters. However, no definitive height estimates are given by the goodness method, therefore no height uncertainties can be either. Instead, at present the user is left to discern how certain any height estimates are that they choose to draw from the colour map. As such, further work could involve producing a single height estimate, with uncertainty, at each timestep using the goodness method.

3 Results and Discussion

3.1 The Intersection Method

Figure 5 shows the time series of the volcanic cloud heights obtained and plotted using the intersection method for the Etna eruptions dated 28/02/21 and 07/03/21. The series show that roughly an hour or longer post-eruption the height estimates for both volcanic clouds settle at an altitude range of approximately 9-11 km. This consistency between two eruptions set only 7 days apart implies that the method is accurate because the LNB of clouds with similar compositions at the same latitude is expected to be consistent. Furthermore, the settled heights are mostly in agreement with the ash heights published by other scientific sources, which are discussed below.

The Toulouse Volcanic Ash Advisory Centre (VAAC) provides updates on volcanic clouds

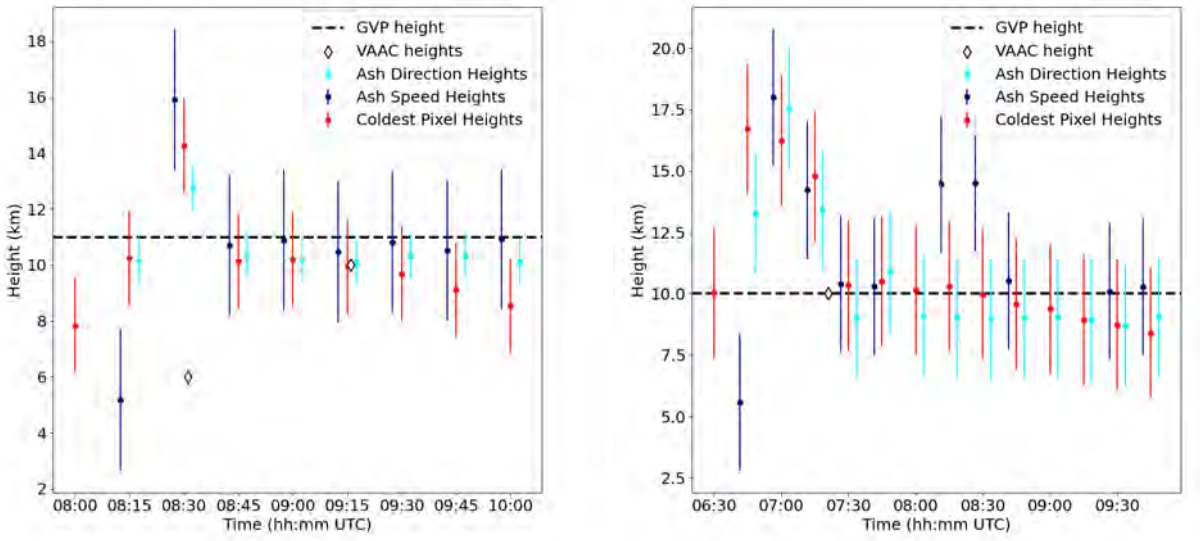

(a) Etna eruption of 28/02/21, starting at 08:00 UTC, with T_{thresh} = 250 K.

(b) Etna eruption of 07/03/21, starting at 06:30 UTC, with T_{thresh} = 230 K.

Figure 5: Time series of the coldest pixel heights, and the closest wind profile ash heights. Absence of a data point indicates that no intersection heights exist at that height. No wind profile data points can be given at the initial timestep as no previous ash location exists to use in calculating the ash speed or direction. Wind profile heights are offset either side of their timestep for ease of viewing.

within their designated VAAC zone. Etna falls within this zone, and so the Toulouse VAAC intermittently report the altitude of Etna's volcanic cloud-tops, often in terms of flight levels, obtained using a combination of satellite imagery and webcams operated by the Instituto Nazionale di Geofisica e Vulcanologia (INGV) [13]. The Smithsonian Institution Global Volcanism Program (GVP) also provides reports on Etna's activity, including the volcanic cloud altitude [14]. This is informed by a variety of sources such as nearby aircraft reports, ground-based images, and satellite instrument imagery. These sources form the pool of validating ash cloud heights.

Scollo et al. [12] state that using the coldest pixel temperature to estimate the volcanic cloud height generally leads to an underestimate of the cloud-top height. This is because the BT method assumes that the cloud is completely opaque. If the cloud isn't completely opaque, some radiation from beneath the cloud is also picked up by the instrument, subsequently measuring a higher BT. Consequently, the cloud height retrieved is lower, where the ambient temperature is slightly warmer.

For the 28/02/21 eruption, the VAAC report a volcanic cloud height of ∼6 km at 08:31 UTC and ∼10 km at 09:16 UTC, and the GVP report an ash cloud altitude of 11 km. For the 07/03/21 eruption, the VAAC report a volcanic cloud height of ∼10 km at 07:21 UTC, and the GVP report agreement with an ash cloud altitude of 10 km. Most of these heights are in agreement with the time series heights within uncertainty, as conveyed in figure 5. Disregarding the stratospheric outliers, the coldest pixel heights for both eruptions are generally equal to or lower than the reported VAAC and GVP heights too, so there also seems to be agreement with Scollo et al. [12]. However, there is disagreement with the 6 km reported at 08:31 UTC 28/02/21 by the VAAC, which highlights some of the problems with the intersection method.

Firstly, both eruption results imply that the ash jumps to stratospheric heights before settling back to the GVP height. The more realistic ash cloud height at 08:30 UTC on 28/02/21 is the 6 km reported by the VAAC because it is physically unlikely that the ash fell ∼4 km in 15 minutes. Consequently, the method seems unsuitable to determine the ash cloud height within the first 45-60 minutes post-eruption. Further inspection shows that there are also only a small number of ash speed heights within 2.5 km of the coldest pixel heights for the 07/03/21 eruption. The ash speed

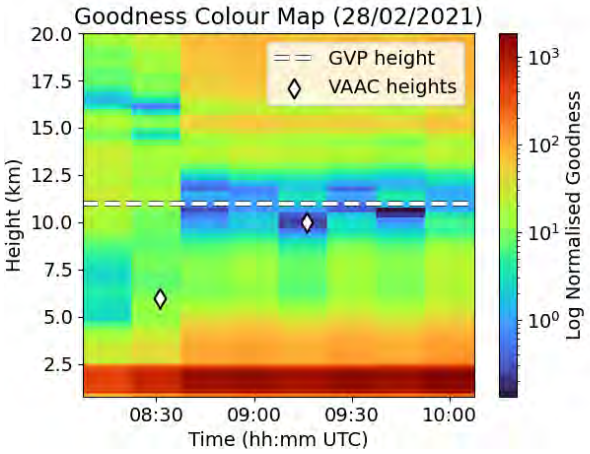

(a) Etna eruption of 28/02/21, starting at 08:00 UTC, with T_{thresh} = 250 K.

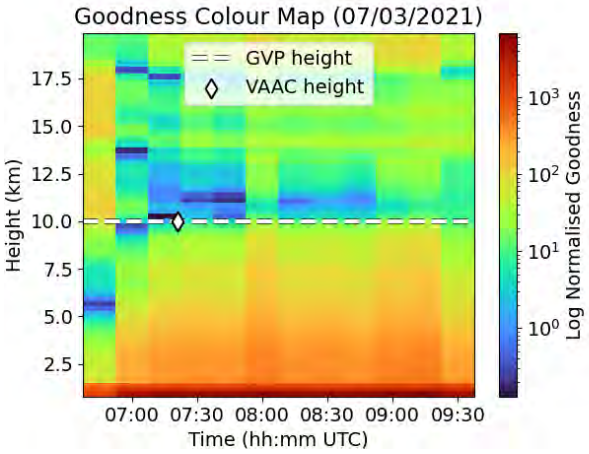

(b) Etna eruption of 07/03/21, starting at 06:30 UTC, with T_{thresh} = 230 K.

Figure 6: Colour maps of the total goodness, G_{tot}, for each height associated with an ERA5 data point across all timesteps processed. Goodness values are logarithmically scaled to better identify altitudes and times with low goodness. Low goodness is associated with good ash height candidates.

heights at 08:15 and 08:30 UTC only agree with the coldest pixel heights within uncertainty because the combined uncertainty ranges of these heights span almost 10 km. Meanwhile, there are no ash speed heights found by the intersection method at 08:00, 09:00, and 09:15 UTC. This is supported by the lack of intersections in the 08:00 UTC wind speed profile in figure 4.

From this it can be argued that: the ash direction is a more consistent indicator of the real ash height than the ash speed for these eruptions; the ash speed and direction do not intersect with the wind speed and direction profiles enough at reasonable ash height estimates to be reliable; and most plotted heights only agree within uncertainty because they are selected based on their closeness to the coldest pixel height. As a result, this method relies too heavily on the coldest pixel height being accurate to be of good use, reducing the usefulness of this method back to confirming whether the ash height is stratospheric or tropospheric [5]. The unreliability within 45-60 minutes of the eruption could be attributed to the cloud not being in thermal equilbrium with the ambient air yet, or to the changing parallax as the ash rises. The goodness method was developed in an attempt to remedy the shortcomings of the intersection method.

3.2 The Goodness Method

Figure 6 shows the colour maps of the total goodness values, G_{tot}, at each height and time for which the ash cloud has been monitored for the eruptions on 28/02/21 and 07/03/21, respectively. Firstly, it should be appreciated that these plots present a broader picture of how the ash and wind profiles behave. For example, it can be observed that the ash cloud is unlikely to be within 2.5 km of the Earth's surface because the wind speed at these altitudes is consistently much lower than the ash cloud speed, like in figure 4. These heights are also physically unlikely because Etna itself has a height of ∼3 km.

Also, the heights of the ash cloud that can be inferred from this data are in agreement with the values provided by the VAAC and GVP, as discussed in section 3.1. These inferred heights are between 10 and 12 km from 08:45 to 10:00 UTC for the 28/02/21 eruption, and between 10 and 11 km from 07:15 to 08:45 UTC for the 07/03/21 eruption. The goodness method heights are also in agreement with the ash direction and coldest pixel heights from the intersection method during these time intervals. However, the more impressive detail is that the colour map for the first eruption implies that the ash could be at a height between 5 and 10 km at 08:31 UTC, when the VAAC reports the height being 6 km. While the goodness is lower at ∼16 km at 08:31 UTC, it is physically unlikely that the ash would fall as significantly as 5 km in 15 minutes, indicating that this is a false positive height estimate. Here, the goodness method benefits by presenting the user with the information to deduce the ash height for themselves.

The user can infer that the most likely ash height

Table 1: Table of limitations, and recommended improvements, to the methods used in this report.

Limitation	Proposed Solution
The wind profile used for comparison is always at Etna, not co-located with the ash.	Spatially interpolate the ERA5 profiles to ash location, or use closest the radiosonde data.
False positive ash pixel flagging is common in high cloud cover scenes (see Figure 7).	Use alternative method for ash detection (e.g. reverse absorption with strict ash threshold) [7][15].
False positive ash pixel flagging fatally moves calculated ash location away from ash cloud (see Figure 7).	Only use flagged pixel shape closest to the last average ash pixel location to calculate the new average ash location.
Higher uncertainty exists in early height estimates while the cloud is rising, therefore parallax from satellite changes the perceived ash cloud location.	Interpolate between the time of eruption and the time to reach the LNB using a plume ascension model to correct heights affected by parallax.
The goodness method provides only a qualitative demonstration of the likelihood that the ash is located at each height.	Define a goodness threshold. Heights at which this threshold is crossed define the uncertainty range of the height estimate.

at 08:31 UTC on 28/02/21 is between 5 and 10 km, and that the estimate is very uncertain because the goodness values are even over this height range. This is a sensible result because the ash at this time will be ascending through different wind regimes, therefore the ash will not consistently be blown in one particular direction. Additionally, the latitude and longitude of the ash cloud still are not easily attributable because the parallax from the instrument to the ash cloud changes with ash height. In conclusion, the colour maps openly demonstrate that the ash-to-wind comparison method is ineffective at determining the ash cloud height within the first 45 minutes post-eruption. This information is extremely useful when deciding how to respond to the ash height, and it would not have been possible to conclude that the ash height is rising in the first 45 minutes of this eruption had all the goodness values not been presented.

The 07/03/21 eruption colour map presents high uncertainty in the height estimates inferred from 09:00 UTC onwards. This could be because ash from this time has begun to fallout from the cloud and enter different wind regimes, thinning or splitting the cloud and making estimates of its height more uncertain. Further evidence of cloud thinning and splitting can be found in appendix C. In addition, the ERA5 wind profiles are spatially interpolated to Etna for all times in this analysis, so the likelihood that the ash responds to a different wind profile increases as the ash moves further from the source. Altogether, these suggest that the goodness method becomes worse at determining the ash height after approximately two hours post-eruption. The effect of the ash moving to a location with worse pixel resolution is considered negligible given the distance traveled by the cloud, on the scale of a few degrees, is small compared to the instrument's longitudinal range of -79 to 79° E.

4 Conclusion

Within this report, the intersection and goodness methods for estimating the height of volcanic clouds were developed and tested on two Mt Etna eruptions from early 2021. It can be concluded that the goodness method has more potential for future application as a volcanic cloud height estimation tool because it does not rely on any other pre-existing height estimation method, and it has proven to more consistently agree with the validation heights provided by the VAAC and GVP. Also, it presents the user with sufficient data to make an informed decision regarding the volcanic cloud height for themselves. However, further development and testing of the goodness method is necessary before implementation as a reliable height estimation tool.

Many of the limitations of the intersection and goodness methods, alongside suggested solutions, are summarised above in table 1. Future work should focus on testing various combinations of these, or other, solutions on height estimation performance for a wider range of eruption types. This is especially important in determining if any relationship exists between the strength of the local wind and energy of the initial eruption; and the accuracy of the goodness method for height esti-

mation and post-eruption delay before height estimations from this method become reliable. That is, understanding the strength of the ash-to-wind coupling for different types of eruption will better define the limitations of this method.

In testing the accuracy of height estimations using ash speeds and directions taken from different satellite instrument images, and wind profiles from sources such as radiosondes, it can be better understood which data sources are most compatible with the goodness method. In this study, all ERA5 profiles were spatially interpolated to Etna, so taking wind profiles from multiple sources could improve horizontal spatial resolution and allow future wind profiles to be accurately interpolated to the longitude and latitude of the ash cloud. Using wind profile sources that take more frequent measurements with altitude would improve the resolution of goodness values in the colour maps and inform more accurate height estimations. However, this must be done while ensuring that the analysis does not become too computationally expensive. With further research and testing, the potential exists for this method to develop into a global, semi-automated ash warning tool.

References

[1] Oxford Economics. *The economic impacts of air travel restrictions due to volcanic ash: A report prepared for Airbus*. 2012. URL: https://controverses.minesparis.psl.eu/public/promo10/promo10_G11/data/documents/Volcanic-Update.pdf.

[2] Global Volcanism Program and R. Wunderman. "Report on Chaitén (Chile)". In: *Bulletin of the Global Volcanism Network, Smithsonian Institution* 33.5 (May 2008). DOI: 10.5479/si.GVP.BGVN200805-358041.

[3] A. Durant, C. Bonadonna, and C. Horwell. "Atmospheric and environmental impacts of volcanic particulates". In: *Elements* 6.4 (2010), pp. 235–240. DOI: 10.2113/gselements.6.4.235.

[4] Y. Zhu et al. "Persisting volcanic ash particles impact stratospheric SO2 lifetime and aerosol optical properties". In: *Nature Communications* 11 (1 2020). ISSN: 2041-1723. DOI: 10.1038/s41467-020-18352-5.

[5] I. Taylor et al. "A satellite chronology of plumes from the April 2021 eruption of La Soufrière, St Vincent". In: *Atmospheric Chemistry and Physics* 23.24 (2023), pp. 15209–15234. DOI: 10.5194/acp-23-15209-2023.

[6] World Meteorological Organization Observing Systems Capability Analysis and Review Tool. *Instrument: SEVIRI*. 2024. URL: https://space.oscar.wmo.int/instruments/view/seviri.

[7] A. J. Prata. "Observations of volcanic ash clouds in the 10-12μm window using AVHRR/2 data". In: *International Journal of Remote Sensing* 10.4-5 (1989), pp. 751–761. DOI: 10.1080/01431168908903916.

[8] F. Prata et al. "The radial spreading of volcanic umbrella clouds deduced from satellite measurements". In: *Volcanica* 8 (Jan. 2025), pp. 1–29. DOI: 10.30909/vol.08.01.0129.

[9] D. Williams. *Earth Fact Sheet*. 2024. URL: https://nssdc.gsfc.nasa.gov/planetary/factsheet/earthfact.html.

[10] European Centre for Medium-Range Weather Forecasts. *Fact Sheet: Reanalysis — ECMWF*. 2023. URL: https://www.ecmwf.int/en/about/media-centre/focus/2023/fact-sheet-reanalysis.

[11] European Centre for Medium-Range Weather Forecasts. *ERA5: data documentation*. 2025. URL: https://confluence.ecmwf.int/display/CKB/ERA5%3A+data+documentation.

[12] S. Scollo et al. "Near-Real-Time Tephra Fallout Assessment at Mt. Etna, Italy". In: *Remote Sensing* 11.24 (2019). ISSN: 2072-4292. DOI: 10.3390/rs11242987.

[13] Meteo-France. *Etna — Toulouse Volcanic Ash Advisory Centre*. 2021. URL: http://vaac.meteo.fr/volcanoes/etna/.

[14] Global Volcanism Program, K. L. Bennis, and E. Venke. "Report on Etna (Italy)". In: *Bulletin of the Global Volcanism Network, Smithsonian Institution* 46.4 (Apr. 2021). DOI: 10.5479/si.GVP.BGVN202104-211060.

[15] A. Kylling et al. "A model sensitivity study of the impact of clouds on satellite detection and retrieval of volcanic ash". In: *Atmospheric Measurement Techniques* 8 (May 2015), pp. 1935–1949. DOI: 10.5194/amt-8-1935-2015.

A Non-Volcanic Cloud Flagging

Figure 7 conveys that for scenes with strong cloud cover, this ash detection method cannot distinguish volcanic from non-volcanic clouds. The analysis method assumes that all flagged pixels within a scene accurately represent the location of the ash. Hence, more thorough ash detection methods should be applied for future use of this analysis method.

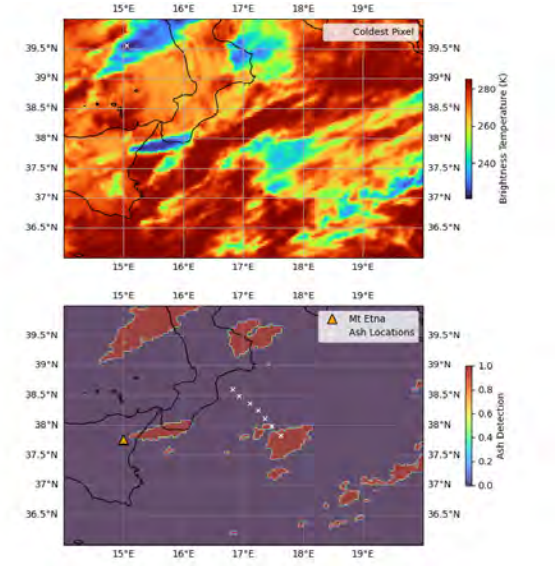

Figure 7: The loaded scene in the vicinity of Etna at 01:30 UTC on 10/03/21. Top: The BT image plotted from SEVIRI's dataset. Bottom: The image of pixels flagged for ash using T_{thresh} = 230 K. At higher BT thresholds, the likelihood of flagging non-volcanic clouds increases. The average ash location at each timestep, denoted by a white cross and calculated as in section 2.3, does not follow the ash motion due to non-volcanic cloud flagging.

B Uncertainty Propagation

The uncertainties introduced by the sub-satellite pixel resolution and the assumption that Earth is spherical are propagated through equations (1) and (2) in order to find the uncertainty in the ash forward bearing, $\delta\beta$, from ash location n to n+1. Firstly, the haversine is decomposed into a North-South surface distance, x, and an East-West surface distance, y, by setting $\Delta\lambda$ and $\Delta\phi$ to zero in the haversine equation (2) respectively, producing equations (7) and (8):

$$x = R\Delta\phi. \tag{7}$$

For the BT image scenes in this report, the maximum latitude range is 5° and the images in appendix C demonstrate that there is little latitudinal ash motion between images. Consequently, the assumption that $\phi_1 = \phi_2$ is made and the subscript is discarded for the East-West surface distance equation:

$$y = 2R\arctan\left(\frac{\cos\phi\sin(\frac{\Delta\lambda}{2})}{\sqrt{1-\cos^2\phi\sin^2(\frac{\Delta\lambda}{2})}}\right). \tag{8}$$

Subsequently, the uncertainties associated with the difference in latitude, $\delta(\Delta\phi)$, and longitude, $\delta(\Delta\lambda)$, between image n and image n+1 are produced by using the variance equations (9) and (10) for propagation of uncertainty through equations (7) and (8), respectively:

$$\delta(\Delta\phi) = \sqrt{\left(\frac{\partial\phi}{\partial R}\right)^2(\delta R)^2 + \left(\frac{\partial\phi}{\partial x}\right)^2(\delta x)^2}. \tag{9}$$

The uncertainties in the Earth surface distances are both set to half the sub-satellite surface pixel resolution, such that $\delta x = \delta y$ = 1.5 km. The uncertainty associated with the change in Earth's radius at different latitudes is conservatively set to the approximate difference between the radius at the equator and at the pole, such that δR = R_e - R_p ≈ 21 km. The uncertainty in the difference of the ash latitude between two images, $\delta(\Delta\phi)$, is directly proportional to the uncertainty in the latitude of the ash cloud in a single image according to $\delta(\Delta\phi) = \sqrt{2}\delta\phi$. Hence, the latitudinal uncertainty is calculated first, as this informs the uncertainty in the difference of the ash longitudes between two images, $\delta(\Delta\lambda)$:

$$\delta(\Delta\lambda) = \sqrt{\left(\frac{\partial\lambda}{\partial R}\right)^2(\delta R)^2 + \left(\frac{\partial\lambda}{\partial y}\right)^2(\delta y)^2 + \left(\frac{\partial\lambda}{\partial\phi}\right)^2(\delta\phi)^2}. \tag{10}$$

Finally, the uncertainty in the forward bearing, $\delta\beta$ can be found by propagating the above uncertainties through equation (1) using equation (11):

$$\delta\beta = \sqrt{\left(\frac{\partial\beta}{\partial\Delta\lambda}\right)^2(\delta(\Delta\lambda))^2 + \left(\left(\frac{\partial\beta}{\partial\phi_1}\right)^2 + \left(\frac{\partial\beta}{\partial\phi_2}\right)^2\right)(\delta\phi)^2}. \tag{11}$$

C BT images of the 28/02/21 and 07/03/21 eruptions of Etna

The following images represent the entire set of scenes, taken from SEVIRI, that are used to find the ash motion variables between each timestep for this report. It can be seen in figures 8 and 10 that the ash cloud is initially optically thick and dense, as demonstrated by the dark blue cloud colour and the smaller size of the low BT region. In later images on both days the ash cloud spreads and thins, as alluded to in section 3.2. Additionally, the 10:00 UTC image in figure 9 and the fourth row of images in figure 11 offer evidence for ash cloud splitting at late times. This splitting could be a result of uneven cooling and/or motion under different wind regimes of different parts of the ash cloud. The ash locations, denoted by white crosses in figures 9 and 11, are determined by averaging over the locations of all flagged pixels in the scene.

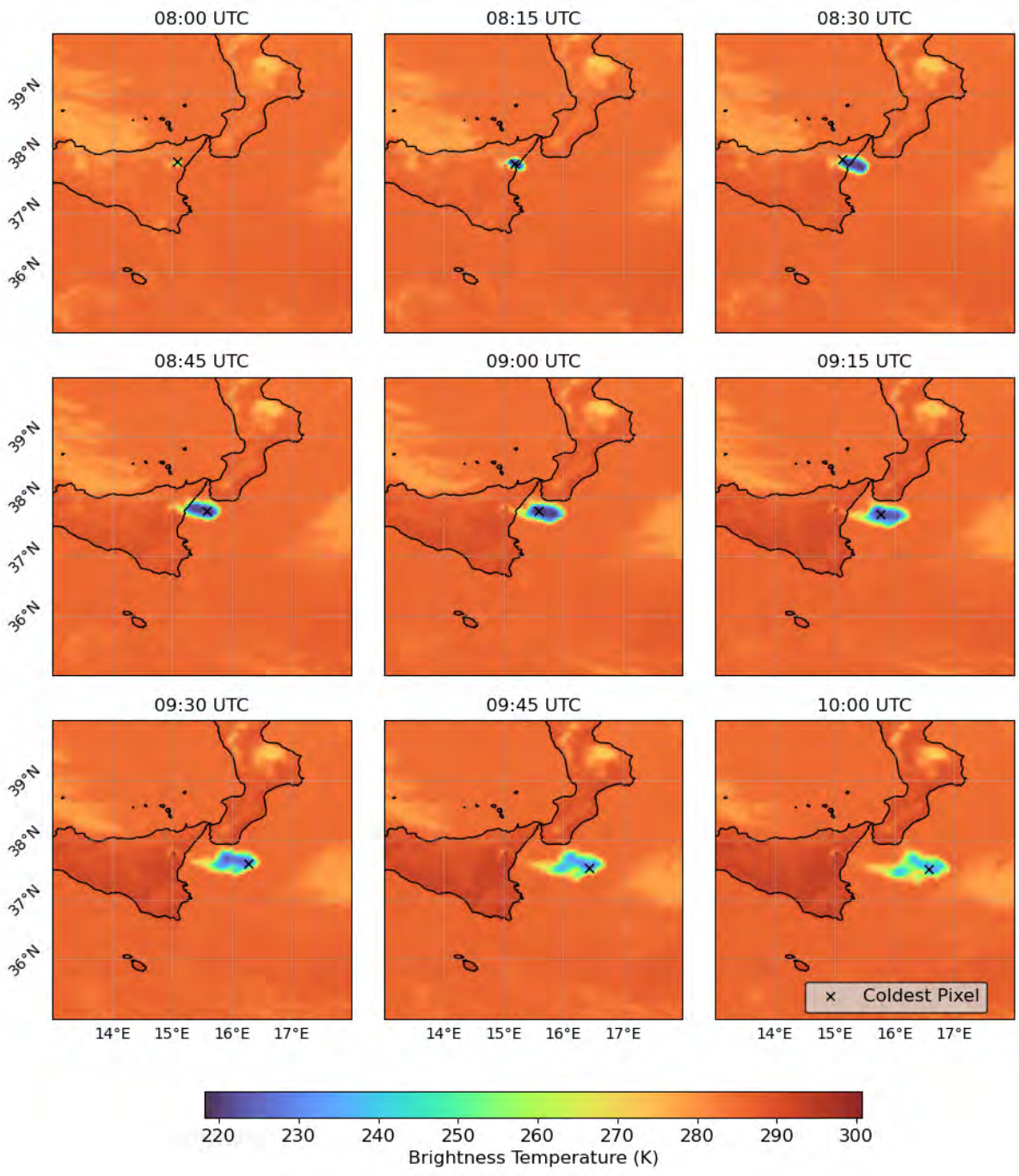

Figure 8: Chronology of the 10.8 μm channel SEVIRI BT images near Etna on 28/02/21, starting at 08:00 UTC.

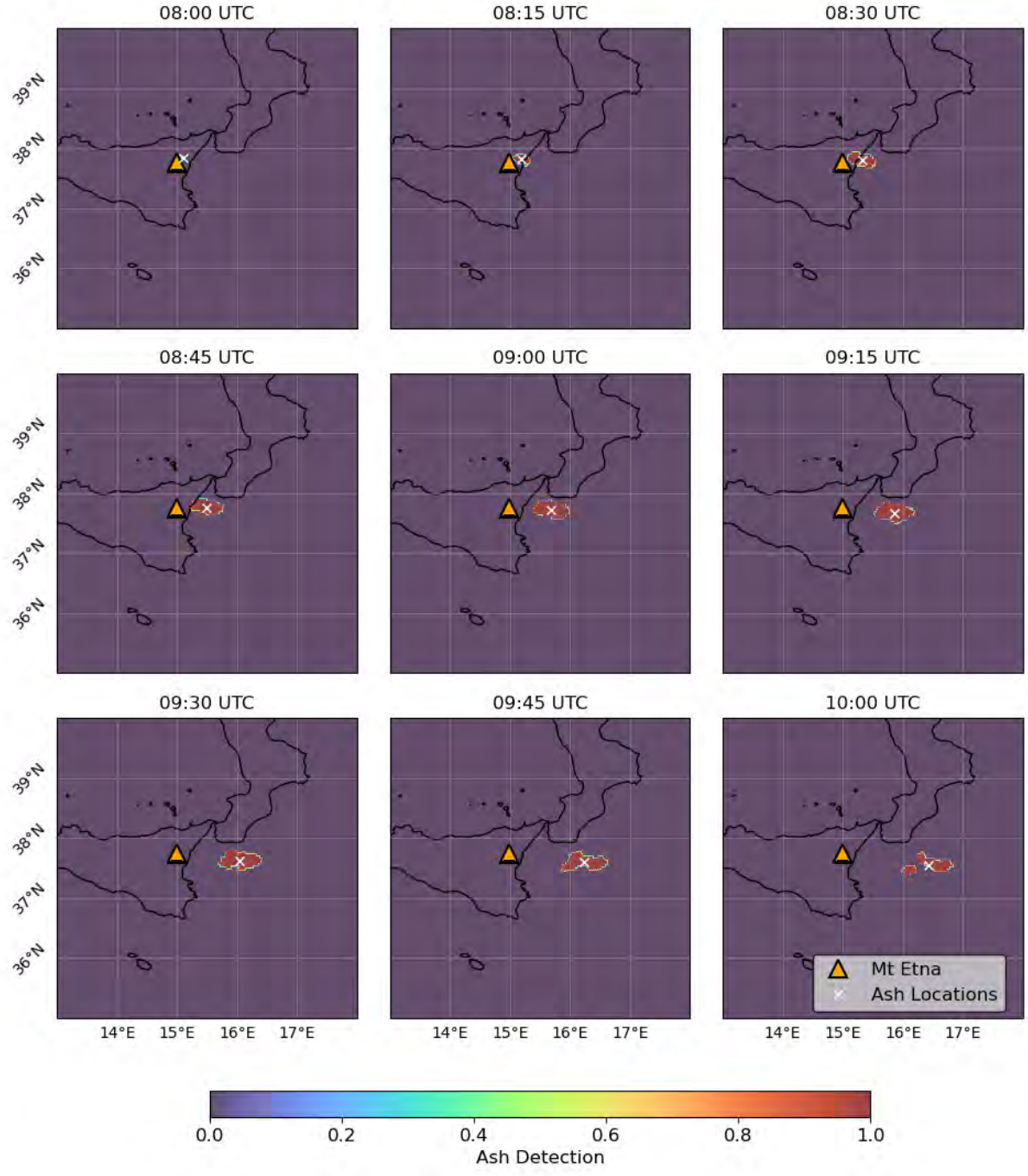

Figure 9: Chronology of the areas flagged for ash near Etna on 28/02/21, starting at 08:00 UTC, with T_{thresh} = 250 K.

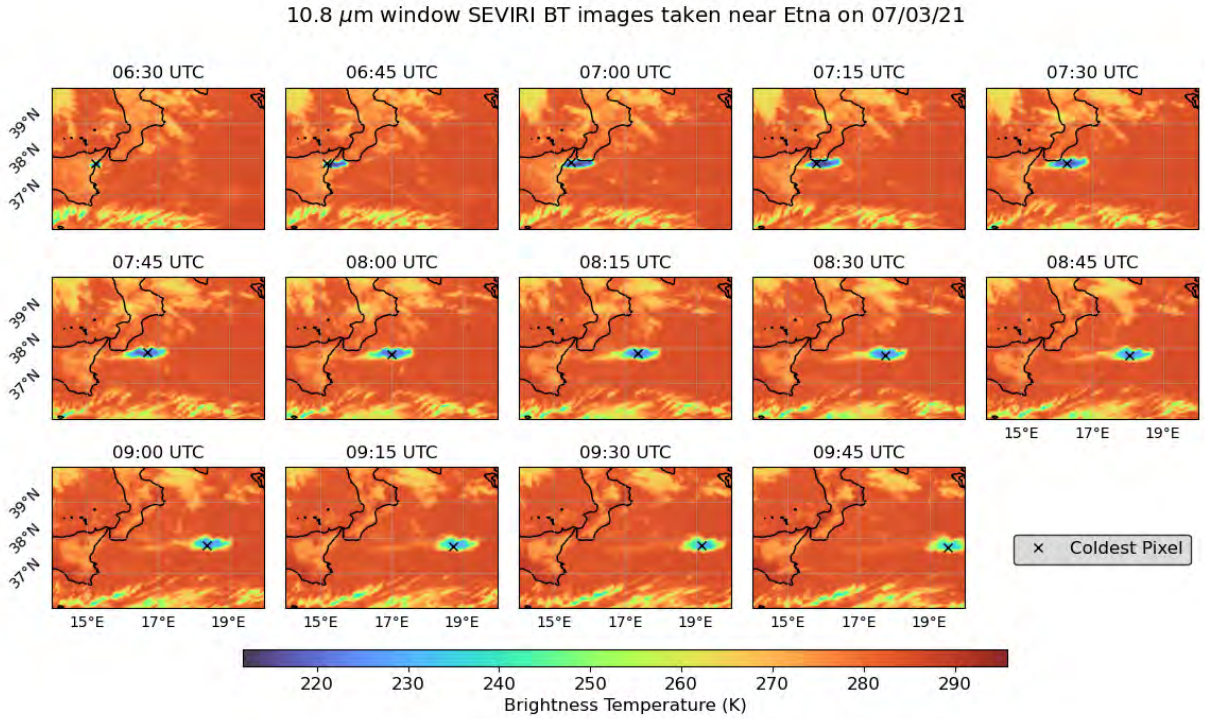

Figure 10: Chronology of the 10.8 μm channel SEVIRI BT images near Etna on 07/03/21, starting at 06:30 UTC.

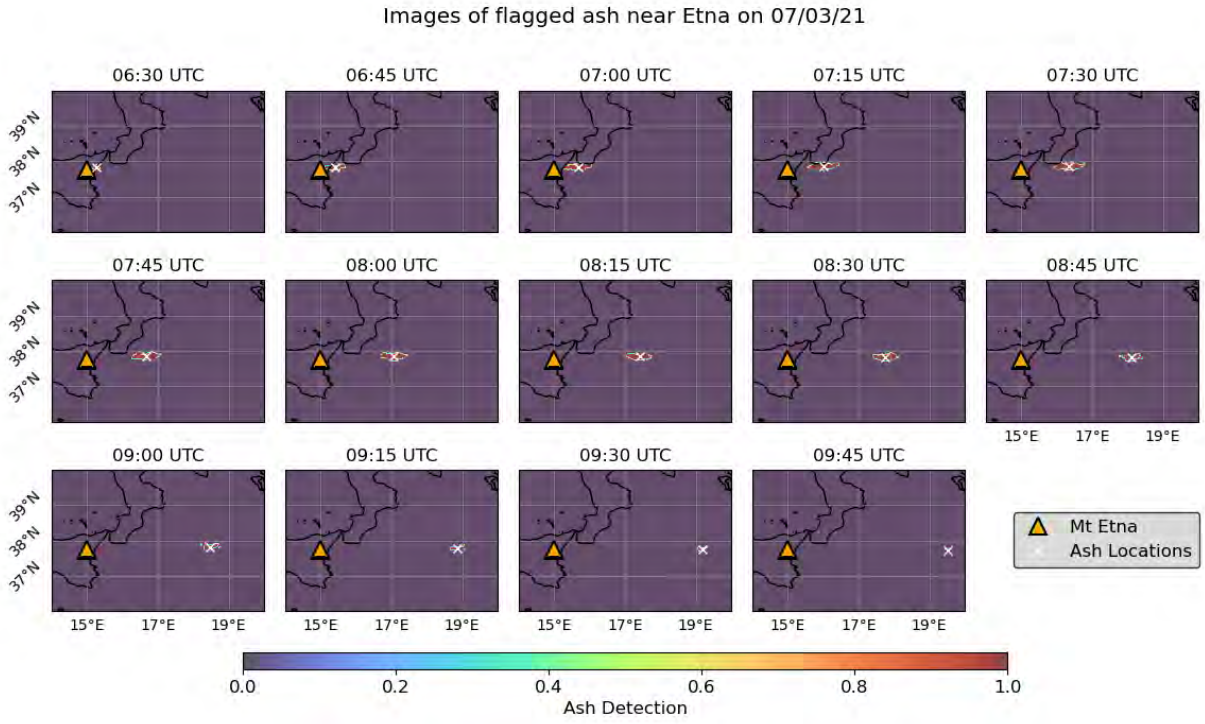

Figure 11: Chronology of the areas flagged for ash near Etna on 07/03/21, starting at 06:30 UTC, with T_{thresh} = 230 K.